Sequential mechanism of solubilization and refolding of stable protein aggregates by a bichaperone network

Pierre Goloubinoff*†, Axel Mogk‡, Anat Peres Ben Zvi*, Toshifumi Tomoyasu‡, and Bernd Bukau†‡

*Silberman Institute of Life Sciences, The Hebrew University of Jerusalem, 91904 Jerusalem, Israel; and ‡Institut für Biochemie und Molekularbiologie, University of Freiburg, Hermann-Herder-Strasse 7, D-79104 Freiburg, Germany

Edited by Alan Fersht, University of Cambridge, Cambridge, United Kingdom, and approved September 29, 1999 (received for review August 3, 1999)

A major activity of molecular chaperones is to prevent aggregation and refold misfolded proteins. However, when allowed to form, protein aggregates are refolded poorly by most chaperones. We show here that the sequential action of two *Escherichia coli* chaperone systems, ClpB and DnaK-DnaJ-GrpE, can efficiently solubilize excess amounts of protein aggregates and refold them into active proteins. Measurements of aggregate turbidity, Congo red, and 4,4′-dianilino-1,1′-binaphthyl-5,5′-disulfonic acid binding, and of the disaggregation/refolding kinetics by using a specific ClpB inhibitor, suggest a mechanism where (*i*) ClpB directly binds protein aggregates, ATP induces structural changes in ClpB, which (*ii*) increase hydrophobic exposure of the aggregates and (*iii*) allow DnaK-DnaJ-GrpE to bind and mediate dissociation and refolding of solubilized polypeptides into native proteins. This efficient mechanism, whereby chaperones can catalytically solubilize and refold a wide variety of large and stable protein aggregates, is a major addition to the molecular arsenal of the cell to cope with protein damage induced by stress or pathological states.

Hsp104 | ClpB | DnaK | Congo red | protein disaggregation

Protein folding in the cell occurs with high efficiency and precision because of the activity of a network of molecular chaperones. Chaperones belong to conserved families of proteins, including the Hsp100 (ClpB, ClpA, ClpX), Hsp90 (HtpG), Hsp70 (DnaK), Hsp60 (GroEL), and α-crystalline-like small heat-shock proteins (IbpA, IbpB) (*Escherichia coli* chaperones in brackets). They share the ability to associate transiently with nonnative protein substrates, which can prevent their aggregation. Some chaperones, including GroEL and DnaK, together with their cochaperones (GroES for GroEL; DnaJ and GrpE for DnaK), hold denatured proteins in nonaggregated states and assist their refolding by a mechanism of recurrent ATPase-driven cycles of substrate binding and release (1).

A biologically important aspect is the fate of proteins that escape the protective activity of chaperones and aggregate. Aggregates form when folding or unfolding intermediates become trapped in partially misfolded states and then successively associate with one another through hydrophobic interactions to become increasingly larger and more stable (2). In the aggregated state, proteins are functionally inactive and enriched in antiparallel β-strands as compared with the native state (3). They are observed as amorphous structures, such as inclusion bodies and heat shock granules, or highly ordered fiber structures, such as amyloid plaques and prions (4). Experimental approaches to observe and operationally define aggregates *in vitro* include sedimentation by low-speed centrifugation, scattering of visible light, and, in the case of amyloid fibers, staining by Congo red (5).

Chaperones in general are poorly efficient at actively dissolving protein aggregates (6–8). Only in isolated cases can GroEL-GroES and DnaK-DnaJ-GrpE (KJE) chaperones with ATP reactivate *in vitro* significant amounts of heat-aggregated RNA polymerase or malate dehydrogenase (MDH), albeit only in the presence of a 10- to 20-fold molar excess of chaperones (7, 9). However, poststress resolubilization of prion-like structures and heat-shock protein granules has been observed in *Saccharomyces cerevisiae* in correlation with the activity of the DnaK-DnaJ and the ClpB homologues, Hsp70-Hsp40 and Hsp104 (10). The participation of these chaperone systems in prevention and solubilization of misfolded proteins probably accounts for the role of Hsp104 in the acquisition of thermotolerance (11). Confirming the genetic evidence, stoichiometric amounts of the combination of yeast Hsp104 and Hsp70-Hsp40 can solubilize and reactivate low-molecular-weight aggregates of luciferase and β-galactosidase *in vitro* (12). In *Thermus thermophilus* the combined action of hexameric *T*$ClpB_6$ and trimeric (*T*$DnaKJ)_3$ chaperones mediates some poststress reactivation of heat-inactivated lactate dehydrogenase, α-glucosidase, and glucose-6-phosphate dehydrogenase (13). However the yields of the reaction are low, with one heat-inactivated substrate molecule recovered by 10 *T*$ClpB_6$ hexamers and as many (*T*$DnaKJ)_3$ trimers. Recovery is only slightly improved when *T*DnaKJ are present during denaturation (13). These observations suggest a noncatalytic mechanism by which $ClpB_6$ assists the refolding of KJE-prebound proteins rather than directs the catalytic rescue of previously stably aggregated proteins formed in the absence of chaperones.

We show here that substoichiometric amounts of the *E. coli* chaperone systems ClpB and KJE act catalytically in the resolubilization and reactivation of a large molar excess of protein aggregates formed in the absence of chaperones. This highly efficient mechanism involves the sequential action of $ClpB_6$, which initially interacts and alters the nature of large and stable protein aggregates, and of KJE, which subsequently disaggregate and refold soluble intermediates into native proteins.

Experimental Procedures

Proteins. Purifications of $ClpB_6$, DnaK, DnaJ, GrpE, GroEL, and IbpB were according to published procedures (5, 7, 14). Pyruvate kinase was from Sigma, and MDH was from Boehringer Mannheim. Protein concentrations were determined by using the Bio-Rad Bradford assay and BSA as standard. Protein concentrations were expressed in protomers, except when ClpB was referred specifically as hexamer and mentioned as $ClpB_6$.

MDH Denaturation. MDH (2 μM) was denatured at 47°C for 30 min in 100 mM Tris, pH 7.5/150 mM KCl/20 mM $Mg(OAc)_2$/10 mM DTT (folding buffer) and diluted to 0.72 μM in the presence of chaperones and ATP. For the MDH dose response in Fig. 1*F*, 14

This paper was submitted directly (Track II) to the PNAS office.

Abbreviations: KJE, DnaK-DnaJ-GrpE; bis-ANS, 4,4′-dianilino-1,1′-binaphthyl-5,5′-disulfonic acid; MDH, malate dehydrogenase.

†To whom correspondence should be addressed. E-mail: pierre@vms.huji.ac.il and bukau@uni-freiburg.de.

The publication costs of this article were defrayed in part by page charge payment. This article must therefore be hereby marked "*advertisement*" in accordance with 18 U.S.C. §1734 solely to indicate this fact.

μM MDH was heat-denatured in folding buffer during 60 min at 47°C and diluted to indicated concentrations and supplemented with ClpB, KJE, and ATP as in Fig. 1*D*.

Chaperone Activity Assay. Aggregated proteins and chaperones were incubated in folding buffer. With the exception of experiments performed with ADP or without nucleotides, all assays were performed in the presence of an ATP-regenerating system of 4 mM phosphoenol pyruvate and 20 ng/ml pyruvate kinase, which was active for the amount of chaperone tested for at least 5 hr at 25°C. MDH reactivation was measured as in ref. 7.

Spectroscopic Measurements. Turbidity was measured in a four-sided quartz cuvette at an excitation and emission wavelength of 550 nm (Perkin–Elmer luminescence spectrometer LS50B). Tryptophan fluorescence of ClpB was measured at 290 nm (excitation) and 340 nm (emission). Fluorescence of 4,4′-dianilino-1,1′-binaphthyl-5,5′-disulfonic acid (bis-ANS) (Molecular Probes) was measured at 340 nm (excitation) and 477 nm (emission). Each sample was equilibrated for 2 min to reach steady-state fluorescence, then measured for 50 sec and averaged. Congo red (Aldrich) binding to aggregated and native MDH (720 nM) was measured from the ratio between absorption at 477 and 540 nm (15, 16) in folding buffer in the presence of 12 μM Congo red.

Quantification of Resolubilized *E. coli* Proteins. *E. coli* cells were grown at 30°C in M9/glucose with all L-amino acids except L-methionine. Labeling was done by adding ^{35}S-labeled methionine (SJ1515; Amersham; 15 mCi/ml, 1,000 Ci/mmol) to 30 μCi/ml cell culture for 2 min, followed by addition of unlabeled L-methionine to 200 mg/ml. After breaking of the cells by a precooled French pressure cell in reaction buffer (50 mM Hepes, pH 7.6/150 mM KCl/20 mM $MgCl_2$/10 mM DTT) and centrifugation (15 min, 15,000 × *g*), the soluble protein extract was adjusted to 4 mg/ml and preincubated for 5 min with ATP (10 mM) at 30°C, then for 15 min at 45°C. Aggregated proteins were collected by centrifugation (15 min at 4°C; 15,000 × *g*). For disaggregation, the washed protein pellet was resuspended and incubated in reaction buffer containing 5 mM ATP, an ATP-regenerating system, 0.33 μM $ClpB_6$, 2 μM DnaK, 0.4 μM DnaJ, and 0.2 μM GrpE. After 4 hr of incubation at 30°C, resolubilized and insoluble proteins were separated by centrifugation as before. Soluble and insoluble ^{35}S-labeled proteins were quantified by scintillation counting. SDS-polyacrylamide gels (12%) (Fig. 4) were loaded with soluble and insoluble proteins and visualized by Coomassie staining.

Results and Discussion

Large and Stable Aggregates of Thermally Denatured MDH as Chaperone Substrates. We used thermally and DTT-denatured MDH as a model system to study the effects of chaperones on aggregates. Heat treatment at 47°C with DTT resulted in the irreversible loss of more than 99% of MDH activity in 30 min. After an initial delay of 5–8 min, the light scattering (turbidity) of the solution increased rapidly as a consequence of formation of large aggregates (Fig. 1*A*). The turbidity and residual enzymatic activity remained constant after a temperature downshift to 25°C for at least 5 hr, demonstrating that heat-inactivated MDH forms stable and irreversible aggregates. Under a phase-contrast microscope, aggregated MDH (2 μM) appeared as loose, reticulated 5- to 50-μm-long filaments (not shown). Gel filtration and SDS-gel electrophoresis of sedimentation-soluble and insoluble fractions (4 min at 14,000 × *g*) showed less than 3% of soluble inactive monomers in the heat-treated MDH sample. In the absence of chaperones, less than 3% of the MDH activity was spontaneously recovered during 24 hr at 25°C. The combined action of KJE and GroEL/GroES chaperones and ATP only recovered some additional 8% from the aggregated MDH in 5 hr and up to 16% in 24 hr (7).

ClpB and KJE Synergistically Disaggregate MDH Aggregates. When applied to MDH aggregates with ATP at 25°C, KJE alone very slowly recovered some small amounts of MDH activity (Fig. 1*D*; 13% in 24 hr). This activity was only slightly improved by supplemented GroEL/GroES (7). Thus, unlike heat-aggregated RNA polymerase (9), a molar excess of KJE and GroEL/GroES chaperones remains ineffective at solubilizing the MDH aggregates. In sharp contrast, when the KJE chaperones were supplemented with ClpB, the turbidity of the MDH solution decreased rapidly (Fig. 1*B*) and the yields of recovered MDH activity reached nearly 100% (Fig. 1*D*). Although the optimal rate of reactivation of aggregated MDH was obtained with an apparent 70-fold molar excess of aggregate over $ClpB_6$ hexamers (Fig. 1*F*), optimal yields of nearly 100% relative to the initial native MDH were obtained at a lower (≤18-fold) molar excess of MDH per $ClpB_6$, prompting us to use in most of our experiments only an 8.6-fold excess of substrate over chaperone. A delay of up to 24 hr before addition of ClpB+KJE, or prolongation of the denaturation time up to 2 hr at 47°C, did not decrease significantly the recovery of native MDH (not shown). Thus, substoichiometric amounts of *E. coli* (ClpB+KJE) chaperones can efficiently disaggregate and reactivate excess molar amounts of large and stable protein aggregates. Our findings extend the initial discovery of a cellular bichaperone system in yeast consisting of Hsp104 and Hsp40/Hsp70 that is able to arrest and revert formation of protein aggregates *in vivo* and *in vitro* (12, 17).

Disaggregation Requires Substoichiometric Amounts of $ClpB_6$ and KJE. The recovery of MDH activity strictly required the presence of both chaperone systems. In particular, ClpB remained ineffective even in the presence of efficient trap chaperones for MDH folding intermediates, such as GroEL or IbpB (not shown), indicating that binding and stabilization of ClpB-modified aggregate by a trap chaperone is not sufficient to drive the disaggregation process. Omission of the cochaperones DnaJ and GrpE resulted in a strong, but incomplete inhibition of disaggregation and reactivation (not shown), pointing to DnaK as the essential partner of ClpB in the reaction.

The rate of enzyme reactivation increased with the concentration of aggregated MDH and reached saturation at a maximal rate of 19 nM min^{-1} at 6 μM MDH, which corresponds to a 72-fold molar excess of MDH monomers over $ClpB_6$ and an 11-fold molar excess over DnaK (Fig. 1*F*). Thus, by actively overcoming the kinetic traps of the protein aggregates, the bichaperone system behaves like a true folding catalyst, whose velocity can be increased and saturated by excess substrate. We determined the ratio between $ClpB_6$ and KJE needed for optimal disaggregation and reactivation of MDH by using the near-linear reactivation rates between 30 and 70 min (Fig. 1*D*). A dose response of $ClpB_6$ in the presence of a fixed optimal amount of KJE reached EC_{50} in the presence of 40 times less $ClpB_6$ (25 nM) than DnaK molecules (Fig. 1*E*). Similarly, a dose response of KJE in the presence of a constant amount of $ClpB_6$ indicated an optimal rate in the presence of 8.4-fold excess of DnaK over $ClpB_6$ (not shown). Thus, substoichiometric amounts of $ClpB_6$ as compared with DnaK, and of DnaK as compared with substrate, are optimal for the reactivation. The mechanism, therefore, is likely to involve highly dynamic interactions between the aggregates and the two chaperone systems. The high efficiency of the *E. coli* bichaperone machinery was affected significantly when components were in nonphysiological, nonoptimal ratios such as equimolar K/J/E. This could account for the observed much lower disaggregation efficiencies initially reported for chaperones from other organisms (12, 13).

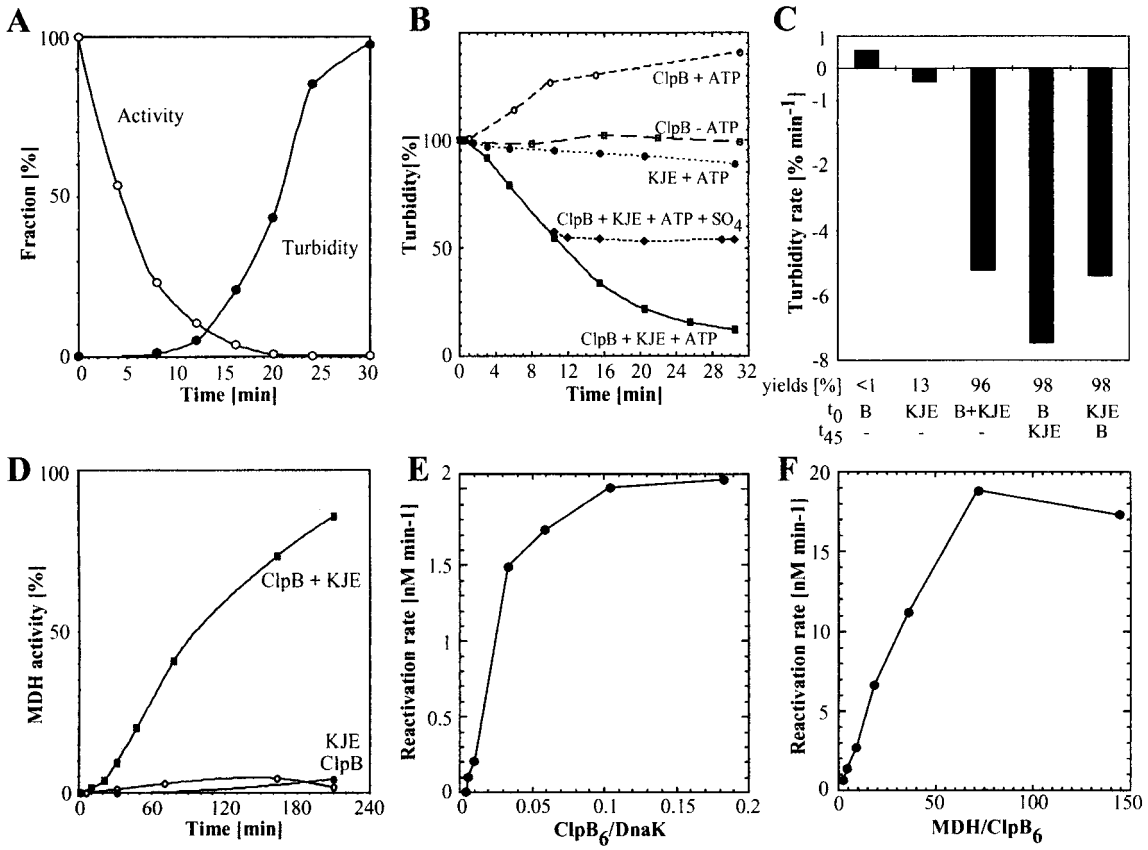

Fig. 1. Aggregation and disaggregation of MDH. (*A*) Time-dependent inactivation and aggregation of 720 nM MDH at 47°C in the absence of chaperones. (*B*) Time-dependent disaggregation at 25°C of heat-aggregated MDH from *A* without or in the presence of supplemented 83 nM $ClpB_6$, 1 μM DnaK, 0.2 μM DnaJ, 0.1 μM GrpE, and 2 mM ATP. $(NH_4)_2SO_4$ (100 mM) was added or not, at $t = 10$ min. Turbidity measured at $t = 1$ min was set as 100%. (*C*) Effect of order-of-addition of $ClpB_6$ and KJE on the rate of MDH disaggregation (as in *B*). Given yields correspond to regained MDH activity after 3-hr incubation at 25°C. (*D*) Time-dependent reactivation of MDH (expressed in percentage of initial native 720 nM MDH) in the presence of ATP, ClpB and/or KJE, as in *B*. (*E*) Effect of increasing concentrations of $ClpB_6$ in presence of constant amounts of KJE and MDH on the rate of MDH reactivation (as in *D*). (*F*) Effect of increasing concentrations of MDH aggregates in the presence of constant amounts of $ClpB_6$ and KJE on the rate of MDH reactivation (as in *D*).

Disaggregation and Reactivation Are Two Sequential Reactions. To dissect the mechanism of disaggregation and refolding, we investigated its kinetics. In the presence of KJE and ClpB, the turbidity rapidly decreased at a rate of 6.5% min^{-1} starting at about 1 min after initiation of the reaction (Fig. 1*C*). In contrast, MDH activity appeared only after a significant delay of 30–45 min, which then increased at a slow rate of 0.7 nM min^{-1} (t_{50} = 100 min, Fig. 1*D*). Thus, disaggregation and reactivation behaved as two distinct sequential reactions, in which the product of an initial rate-determining disaggregation reaction served as the substrate for a subsequent refolding reaction.

Further evidence for a stepwise disaggregation reaction was obtained by centrifugation of MDH aggregates. Disaggregation and reactivation of MDH were inhibited by centrifugation, probably because of the reduction of accessible surfaces in MDH aggregates for the chaperones in solution (Fig. 2). Noticeably, even when applied 60 min after initiation of the reaction, centrifugation still strongly inhibited the reactivation, although the reaction was largely devoid of turbid particles (Fig. 1*B*). This indicates that the substrate of the disaggregation reaction varies with time, from a population of large and turbid aggregates in the first phase of the reaction (0–30 min), to smaller, nonturbid yet centrifugable aggregates in the later phases of the reaction (>30 min).

Several lines of evidence indicate that ClpB acts before the KJE system in the disaggregation mechanism. First, in the presence of ClpB and ATP, but not without ATP, the turbidity of the aggregated protein solution increased slowly (Fig. 1*B*) and nearly doubled within 3 hr (not shown). Because less than 3% monomeric MDH is present in the aggregate fraction, this increase in turbidity can be attributed either to an increase in the size of the particles or to the partial fragmentation of very large aggregates into smaller, but possibly better substrate particles for subsequent KJE-mediated disaggregation. ClpB alone thus induced conformational changes in the aggregates in an ATP-dependent manner.

Second, we discovered a specific inhibitor of ClpB that allowed to functionally differentiate between ClpB and KJE. Disaggregation and reactivation of aggregated MDH were strongly inhibited by 100 mM $(NH_4)_2SO_4$ (Figs. 1*B* and 2) (half-maximal inhibition by 40 mM) whereas 100 mM NH_4Cl remained without effect. This inhibition by SO_4^{-2} ions is specific for ClpB, because a KJE-dependent refolding reaction of heat denatured MDH, in which KJE without ClpB were added before aggregation, was even slightly more efficient in the presence of 100 mM $(NH_4)_2SO_4$ (120%, not shown). Consequently, when sulfate was added in the MDH disaggregation reaction at $t = 0$, the yield of reactivated MDH after 5 hr was 94% lower than that without sulfate. When added at $t = 15$ min, the yield was already half that of maximal yield without sulfate, whereas an addition at 30 min had no effect on the yield (Fig. 2). ClpB activity thus is rate-determining only during the first phase of the reaction, where large, turbid protein aggregates are converted into smaller, nonturbid aggregates. Because ClpB is not limiting for

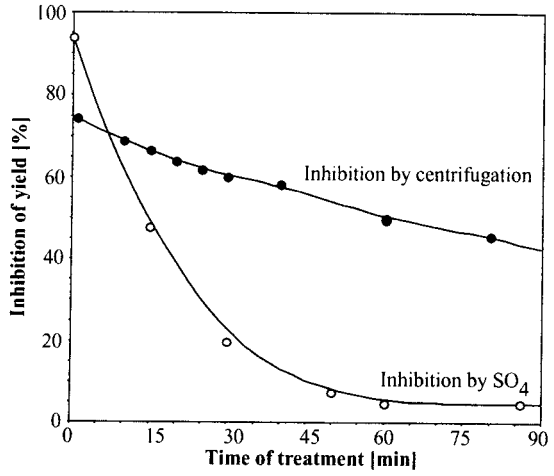

Fig. 2. Inhibition of MDH disaggregation by sulfate and centrifugation. (ClpB+KJE)-mediated MDH reactivation as in Fig. 1 was measured after 270 min. Addition of 100 mM $(NH_4)_2SO_4$ or centrifugation (3 min, 16,000 × *g*) was performed at indicated time points. Inhibition of reactivation was expressed as percent loss of recovered MDH activity as compared with the activity without inhibition at 270 min.

the reactions beyond 30 min, this implies that the KJE system alone is capable of converting small, nonturbid aggregates into soluble and active enzymes.

ClpB Alters the Nature of the Protein Aggregates. Our conclusions were substantiated further by order-of-addition experiments. When the aggregates were preincubated for 45 min with KJE and ATP, then supplemented with ClpB, disaggregation initiated at the same rate as when ClpB and KJE were added concomitantly. In contrast, when the aggregates were preincubated for 45 min with ClpB and ATP, then supplemented with KJE, disaggregation was 1.3-fold faster than when ClpB and KJE were added concomitantly (Fig. 1*C*). Noticeably, a longer preincubation (3 hr) with ClpB and ATP decreased the rate of disaggregation upon KJE addition (not shown), emphasizing the transient nature of the ClpB-induced changes in the aggregate, perhaps through ClpB-mediated increases in aggregate size. When the aggregates were preincubated for 45 min first with ClpB and ATP, then supplemented with KJE and 100 mM $(NH_4)_2SO_4$, disaggregation did not occur (not shown). Thus, although ClpB alone can change the nature of large aggregates in an ATP-dependent manner, the concomitant action of ClpB and KJE remains essential to their solubilization into nonturbid aggregates.

We investigated whether the disaggregation reaction is a passive process resulting from the chaperone-mediated removal of dissociated monomers from the equilibrium or an active process in which ClpB directly interacts with the aggregates and solubilizes them in cooperation with KJE. We first observed that there is no significant disaggregation when free MDH species (about 3%) are removed by gel filtration (not shown) or by the active refolding by KJE or GroEL/GroES chaperones (7). Second, we investigated the nature of the changes in the aggregates caused by ClpB and ATP by using fluorescence spectroscopy. MDH aggregates bound about 3-fold more molecules of the hydrophobicity probe bis-ANS and one to two orders of magnitude more molecules of the structural probe Congo red, which associates with β-sheets, as compared with native MDH. Thus, similar to amyloid plaques (15), heat-denatured proteins also show increased hydrophobic surfaces and bind Congo red. When aggregated MDH was incubated with ClpB and ATP, bis-ANS binding increased rapidly by 22% within the first 30 min

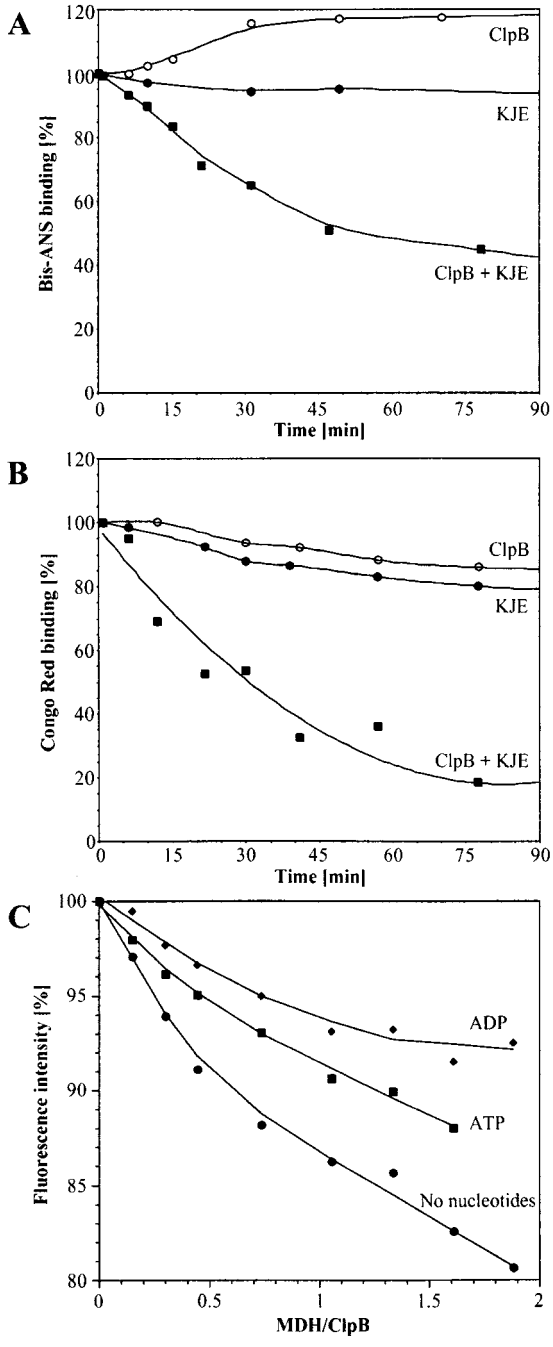

Fig. 3. Modulation of interaction and ClpB-induced conformational changes in heat-aggregated MDH. Time-dependent change in bis-ANS binding (*A*) and Congo red binding (*B*) to heat-aggregated MDH after incubation with ATP, ClpB and/or KJE as in Fig. 1*B*. bis-ANS and Congo red binding to aggregated MDH before chaperone addition is set as 100%; baseline binding levels in native MDH is set as 0%. (*C*) Interaction of $ClpB_6$ with MDH aggregates and nucleotides by Trp fluorescence. Effects of increasing concentrations of aggregated MDH on the intrinsic fluorescence intensity of $ClpB_6$ (83 nM) without or with 3 mM ATP or ADP.

(Fig. 3*A*), whereas Congo red binding decreased slowly (Fig. 3*B*). This increase in hydrophobicity, together with the observed slow increase in turbidity of the aggregates in presence of ClpB and ATP (Fig. 1*B*), demonstrates that ClpB alters the structure of the aggregate in an ATP-dependent manner by exposing more hydrophobic surfaces in the aggregates, which renders them more prone to further aggregation. When aggregated MDH was

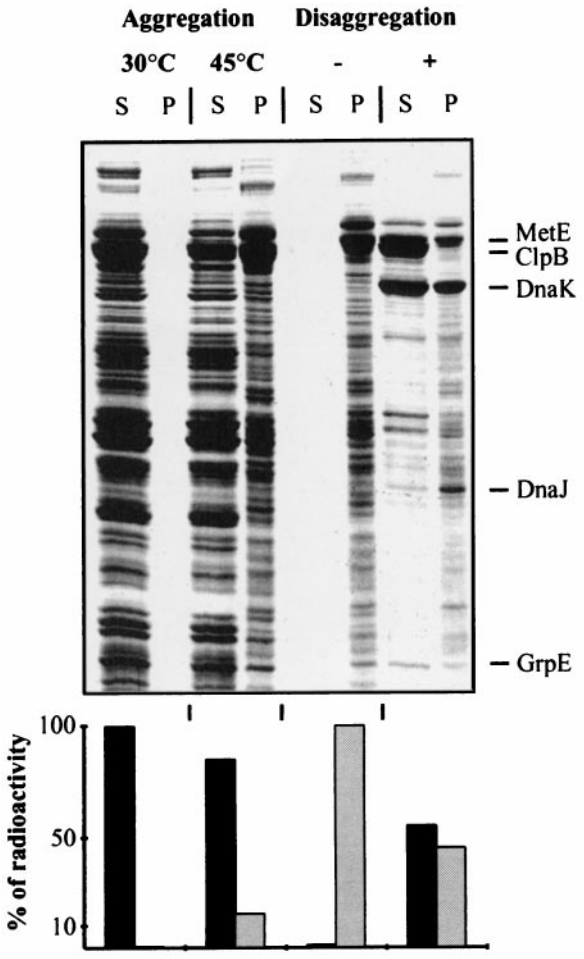

Fig. 4. Solubilization of a wide range of heat-aggregated proteins. Soluble ^{35}S-labeled protein extracts from wild-type *E. coli* cells (MC4100) were aggregated at 45°C and incubated for 4 hr with ATP, ClpB, and KJE (see *Experimental Procedures*). Resolubilized and aggregated proteins were separated by centrifugation. Gels were loaded with equal volumes, such that the insoluble fractions were 2.5-fold more concentrated relative to the soluble fractions. Soluble (S) and aggregated (P) proteins were analyzed by Coomassie staining (*Upper*) and quantified by scintillation counting (*Lower*).

incubated with ClpB and KJE in the presence of ATP, binding of bis-ANS and Congo red decreased at similar rates (1.3 and 1.8% min^{-1}, respectively, Fig. 3), which were 3- to 4-fold slower than the rate of turbidity decrease (Fig. 1*B*), confirming that disaggregation continues beyond the first 30 min. Thus, during disaggregation and refolding, ClpB and KJE modify in successive actions two central structural characteristics of increased hydrophobic exposure and higher β-sheet content, shared by amyloid plaques, prion particles, and now also by heat-induced aggregates.

ClpB Interacts Directly with Aggregates of MDH. We took advantage of the lack of tryptophans in MDH to investigate whether ClpB interacts directly with protein aggregates. Although real affinity values cannot be calculated from such an experiment because the substrate is largely insoluble, it allowed qualitative detection of fluorescence changes. A dose response of aggregated MDH in the presence of $ClpB_6$ hexamers under steady-state conditions showed a strong decrease in the intrinsic fluorescence of ClpB (Fig. 3*C*). The fluorescence change was strongest without nucleotides and decreased with ATP and even more with ADP. These findings suggest that ClpB in the absence of added nucleotide has an affinity for the aggregate, which is decreased upon nucleotide binding. However, further kinetic analysis is required to assign more precisely the roles of individual nucleotide states for ClpB activity. Fluorescence spectroscopy also revealed that ClpB, without added nucleotides or in the presence of ATP, binds 40% and 50% more bis-ANS, respectively, than in the presence of ADP. This indicates that ClpB then exposes more hydrophobic surfaces, which possibly interact with exposed hydrophobic regions in protein aggregates.

Generality of the ClpB+KJE Bichaperone System. To evaluate the generality of the MDH-disaggregating activity of *E. coli* ClpB and KJE, we tested substrate specificity with additional model substrates. Heat-aggregated forms of firefly luciferase, glucose-6-phosphate dehydrogenase, and α-glucosidase all were disaggregated and reactivated by the *E. coli* bichaperone system, albeit at somewhat lower rates and yields than MDH (not shown). In contrast, the bichaperone system was found to efficiently disaggregate a large array of natural *E. coli* substrates, similar to mitochondrial MDH. When the soluble protein fraction from *E. coli* was incubated at 45°C, about 15% of total protein stably aggregated within 15 min (Fig. 4). Incubation of the aggregated fraction with ATP, ClpB, and KJE, but not ClpB or KJE (not shown), resulted in the solubilization of about 55% of the amount of aggregated proteins within 4 hr (Fig. 4). At least 150 different proteins of various sizes were resolubilized to various extents (A.M. and B.B., unpublished data). Noticeably, the KJE system solubilized only a minor fraction (5–6%) of the aggregated proteins, indicating that it can act only on a subset of protein aggregates in the cell, possibly the very small aggregates. Thus, the (ClpB+KJE) bichaperone system can disaggregate and reactivate a wide spectrum of natural substrates, albeit with various efficiencies, which may depend on the size and nature of the aggregates.

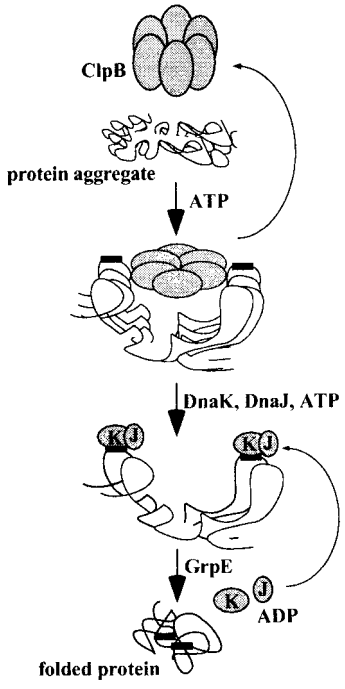

Fig. 5. Model for the sequential action of ClpB and KJE. ClpB binds protein aggregates. ATP-driven changes in the structure of ClpB expose new hydrophobic sites in ClpB-bound aggregates. This allows binding of KJE and mediating of disaggregation and refolding of the aggregated protein.

Conclusion

Based on spectroscopic and kinetic observations of the disaggregation and reactivation reactions, we propose a mechanism in which (*i*) the $ClpB_6$ ring directly binds protein aggregates, (*ii*) ATP induces structural changes in the $ClpB_6$ ring that shear the aggregates and expose new hydrophobic regions, and (*iii*) the resulting transient increase in hydrophobic exposure allows KJE to bind and mediate dissociation of aggregates and to refold solubilized polypeptides into native proteins (Fig. 5).

Several conclusions can be reached about the nature of the aggregates before and during the bichaperone-mediated reaction. At $t = 0$, the aggregate is composed of larger particles that scatter light and smaller particles that do not. Yet, both types of particles can be centrifuged (97%) and strictly require ClpB and KJE for reactivation. The large, turbid particles are rapidly (30 min) converted into smaller, nonturbid particles but remain large enough to be centrifuged. This initial step is likely to be a fragmentation process with a strong effect on light scattering but limited effects on the intrinsic nature of the aggregates in terms of hydrophobic exposure and Congo red binding. SO_4^{-2} inhibition demonstrates that the initial fragmentation process of the large particles is strictly dependent on ClpB+KJE, whereas subsequent changes in the intrinsic nature of the smaller aggregates (hydrophobic exposure and Congo red binding) and enzyme reactivation can be carried out by the KJE system alone.

Such chaperone-mediated protein disaggregation has significant biological relevance, as shown previously for yeast (11, 17). Under stress conditions, including heat shock, and during recovery from stress, *E. coli* cells may survive for days without dividing. Such conditions would provide the ClpB+KJE bichaperone system sufficient time to disaggregate proteins in the cell, and a 2-hr half-time for recovery of aggregated MDH (Fig. 1*C*) therefore can be a physiologically relevant time frame.

It is interesting that in [*PSI*$^+$] yeast cells, which accumulate aggregates of a prion-like protein, Sup35, different expression levels of Hsp104 can either promote or solubilize these particles (10, 18). We show here that heat-induced MDH aggregates share with amyloid and prion aggregates the ability to bind significantly more Congo red and bis-ANS than the native conformers. In addition, if ClpB is present in large excess, or present without KJE (Fig. 1*B*), protein aggregation can increase rather than decrease. It is thus an intriguing possibility that not only solubilization but also formation of protein aggregates, including prion and amyloid plaques, are modulated by the balance between the components of the bichaperone system. It is tempting to speculate that despite the absence of ClpB homologues in animal cells, a mechanistically similar chaperone network exists that removes toxic aggregates. After acute stress, or when chaperones are poorly expressed during aging, such chaperone network may become overwhelmed and allow critical concentrations of toxic conformers to seed prion and amyloid formation. By preventing and actively solubilizing protein aggregates, chaperones may serve as a central mechanism of protection against diseases and aging processes linked to protein misfolding.

We thank C. Squires for plasmid pClpB, A. Jacobi and M. Mayer for purified chaperones, and laboratory members for help and discussions. This work was supported by grants from the Alexander von Humboldt Stiftung to P.G., the Abish-Frenkel Foundation to A.P.Z., and the Deutsche Forschungsgemeinschaft and the Fonds der Chemie to B.B.

1. Bukau, B. & Horwich, A. L. (1998) *Cell* **92,** 351–366.
2. Jaenicke, R. (1998) *Biol. Chem.* **379,** 237–243.
3. Turnell, W. G. & Finch, J. T. (1992) *J. Mol. Biol.* **227,** 1205–1223.
4. Horwich, A. L. & Weissman, J. S. (1997) *Cell* **89,** 495–510.
5. Woo, K. M., Kim, K. I., Goldberg, A. L., Ha, D. B. & Chung, C. H. (1992) *J. Biol. Chem.* **267,** 20429–20434.
6. Goloubinoff, P., Christeller, J. T., Gatenby, A. A. & Lorimer, G. H. (1989) *Nature (London)* **342,** 884–889.
7. Veinger, L., Diamant, S., Buchner, J. & Goloubinoff, P. (1998) *J. Biol. Chem.* **273,** 11032–11037.
8. Schröder, H., Langer, T., Hartl, F.-U. & Bukau, B. (1993) *EMBO J.* **12,** 4137–4144.
9. Ziemienowicz, A., Skowyra, D., Zeilstra-Ryalls, J., Fayet, O., Georgopoulos, C. & Zylicz, M. (1993) *J. Biol. Chem.* **268,** 25425–25431.
10. Patino, M. M., Liu, J.-J., Glover, J. R. & Lindquist, S. (1996) *Science* **273,** 622–626.
11. Sanchez, Y., Taulin, J., Borkovich, K. A. & Lindquist, S. (1992) *EMBO J.* **11,** 2357–2364.
12. Glover, J. R. & Lindquist, S. (1998) *Cell* **94,** 73–82.
13. Motohashi, K., Watanabe, Y., Yohda, M. & Yoshida, M. (1999) *Proc. Natl. Acad. Sci. USA* **96,** 7184–7189.
14. Laufen, T., Mayer, M. P., Beisel, C., Klostermeier, D., Reinstein, J. & Bukau, B. (1999) *Proc. Natl. Acad. Sci. USA* **96,** 5452–5457.
15. Klunk, W. E., Pettegrew, J. W. & Abraham, D. J. (1989) *J. Histochem. Cytochem.* **37,** 1273–1281.
16. Klunk, W. E., Pettegrew, J. W. & Abraham, D. J. (1989) *J. Histochem. Cytochem.* **37,** 1293–1297.
17. Parsell, D. A., Kowal, A. S., Singer, M. A. & Lindquist, S. (1994) *Nature (London)* **372,** 475–478.
18. Chernoff, Y. O., Lindquist, S. L., Ono, B.-i., Inge-Vechtomov, S. G. & Liebman, S. W. (1995) *Science* **268,** 880–884.